Simulations of the Holocene Climate in Europe Using Dynamical Downscaling within the iLOVECLIM model (version 1.1)

Frank Arthur[1] , Didier M. Roche[2,3], Ralph Fyfe[4] , Aurélien Quiquet[3] , Hans Renssen[1]

[1]Department of Natural Sciences and Environmental Health, University of South-Eastern Norway, Bø, Norway**.**

5   [2]Faculty of Science, Cluster Earth and Climate, Vrije Universiteit Amsterdam, Amsterdam, the Netherlands.

[3]Laboratoire des Sciences du Climat et de l'Environnement, LSCE/IPSL, CEA-CNRS-UVSQ, Université Paris-Saclay Gif-sur-Yvette, France.

[4]School of Geography, Earth and Environmental Sciences, University of Plymouth, Plymouth, UK**.**

Correspondence to: Frank Arthur (Frank.Arthur@usn.no)

10   **Abstract.** This study presents the application of dynamical downscaling in Europe using iLOVECLIM (a model of intermediate complexity), increasing its resolution from 5.56° to 0.25° latitude-longitude. A transient simulation using the appropriate climate forcings for the entire Holocene (11.5 – 0 kyr BP) was done for both the standard version of the model and with dynamical downscaling applied. Our results show that, simulations from dynamical downscaling present spatial variability which agrees better with proxy-based reconstruction and other climate models as compared to the standard model.

15   The downscaling scheme simulates much higher (by at least a factor of two) precipitation maxima and provides detailed information in mountainous regions. We focus on examples from the Scandes Mountains, the Alps, the Scottish Highlands and the Mediterranean. The higher spatial resolution of the dynamical downscaling provides a more realistic overview of the topography, gives local climate information such as precipitation and temperature gradient that is important for paleoclimate studies. The results from the downscaling show in some cases similar magnitude of the precipitation changes reconstructed by

20   other proxy studies (for example in the Alps). There is also a good agreement for the overall trend and spatial pattern than the standard version. Our downscaling tool is numerically cheap which can perform kilometric-multi-millennial simulations and suitable for future studies.

25   **1.0 Introduction**

Numerical climate models are used to study the past, present and future climate change, two types of global climate models are primarily used, the so-called General Circulation Models (GCMs) and Earth System Model of Intermediate Complexity (EMICs). GCMs and EMICs simulate the climate of the Earth by applying mathematical equations to describe the atmospheric,

30   oceanic and land interactions or feedbacks. These climate models are evaluated with past climate data to ensure that their sensitivity to climate change is realistic, and thus improve their ability to project future climate change. GCMs and EMICs

have been used to simulate the past climate. For example, the Last Glacial Maximum (e.g., Liu et al., 2011), the Holocene (e.g., Claussen et al., 2002; Goosse and Fichefet, 2009; Renssen and Osborn, 2003; Schmidt et al., 2004; Otto-Bliesner et al., 2006), and the Last Millennium (e.g., Crowley, 200; Jones et al., 2001; Zorita et al., 2005). These paleoclimate simulations

35   have been routinely compared with proxy-based paleo data to evaluate their performance (Masson et al., 1999; Bonfils et al., 2004; Brewer et al., 2007; Bartlein et al., 2011). However, the difference in spatial resolution between the simulated climate model results and proxy-based paleo reconstructions makes this comparison problematic and usually poses some uncertainties (Renssen et al., 2001; Ludwig et al., 2019). Transient simulations of the Holocene with GCMs are still currently a challenge due to the numerical cost (it can take more than 4-5 months). Therefore, EMIC's tools like iLOVECLIM which have a

40   simplified physics are more efficient, making it feasible to perform large ensemble experiments at a multi-millennial timescale, which can be an advantage to paleoclimate studies. EMICs can simulate explicitly the interaction between all the components of an earth system model and simulate the transient and equilibrium climate sensitivity (Claussen et al., 2002). Still, EMICs' representation of the large-scale atmospheric moisture content and other processes produced by local scale features such as mountains ranges, water bodies, forest etc. is quite poor and thus affecting the dynamics of these sub-components that rely on

45   the global atmospheric water cycle (Quiquet et al., 2018). This implies that many of the processes that govern the local climate (vegetation, hydrology and topography) are not well represented in most EMICs' coarse resolution (Viner, 2012).

This limitation of global climate models can be overcome by applying spatial downscaling, a primary tool in meteorology and climate studies. Downscaling can establish a relationship between large-scale atmospheric processes and the local scale to

50   derive information at a fine spatial resolution (Castro et al., 2005). There are two approaches of downscaling used to resolve this coarse-fine resolution variance: statistical and dynamical downscaling (Murphy, 1999). Statistical downscaling involves creating an empirical relationship between historical large-scale atmospheric characteristics (such as pressure fields) and local climate variables (temperature, precipitation, etc.), and applying these statistical relationships to the output of large-scale global variables (GCMs/EMICs) to simulate the local climate variables (e.g., Stoner et al., 2012). Dynamical downscaling is the

55   technique used by global models to simulate the land-atmosphere interaction process by considering the sub-grid, orography and other conditions over a local scale (Feser et al., 2011). In this approach, precipitation, temperature, relative humidity, and other climatic variables are physically recomputed on a fine spatial resolution based on the output from the coarse native atmospheric component.

60   Dynamical downscaling is thus aimed at increasing the spatial resolution (horizontally and vertically) by simulating the regional sub-component of the climate from global models (Ludwig et al., 2019). In contrast, statistical downscaling only assumes constant statistical relationships between large and local-scale processes. These relationships may not be valid for conditions very different from the present, such as in the early Holocene. Conversely, since it is based on physical laws, dynamical downscaling can be applied to any period and gives more comprehensive information for some specific regions

65   (Feser et al., 2011), particularly if precipitation is highly influenced by local topography (Gomez-Navarro et al., 2011; Wang

et al., 2015; Raible et al., 2017; Quiquet et al., 2018). However, there may be some uncertainties and limitations in the use of dynamical spatial downscaling. The uncertainties of downscaled temperature and precipitation usually depend on the errors associated with the large-scale model such as its physical parameterization (Murphy, 1999; Feser et al., 2011), the model's simplification or limitation and the biases associated with the model's atmospheric circulation (Quiquet et al., 2018).

70

Comparing paleoclimate model results at a high spatial resolution with proxy-based data informs meaningful interpretation (Bonfils et al., 2004; Russo and Cubasch, 2016; Ludwig et al., 2019). Dynamical downscaling has been applied on both present and future climate analyses to give an improved estimate of future climate change (e.g., Jacob et al., 2007). According to Jacob et al. (2014), regional (dynamical) downscaling better represents the physical processes that trigger precipitation and provides

75   more realistic outputs in complex regions when compared to outputs from low-resolution models. Despite these advantages, applying dynamical downscaling in paleoclimate studies is still limited; the main reason is that it is computationally intensive and costly to run long-term climate simulations with downscaling. Still, there is good potential, as comparing paleoclimate simulations with proxy-based reconstructions is more meaningful at a high spatial resolution.

80   Some attempts have been made in the past to simulate high-resolution climate in a paleo-perspective. Examples are available for the Last Glacial Maximum (Yokoyama et al., 2000; Strandberg et al., 2011) and the Little Ice Age/Medieval Warm Period over arid central Asia (Fallah et al., 2016), the Last Millennium over the Iberian Peninsula (Gomez-Navarro et al., 2011). Renssen et al. (2001) also applied Regional Climate Modelling to simulate the European climate during the Younger Dryas cold period (12.9-11.7 thousand years before present, kyr BP). Here we apply for the first time a dynamical downscaling to an

85   Earth system model of intermediate complexity (i.e., iLOVECLIM) to perform transient simulations of the Holocene climate in Europe (Fig. 1).

The Holocene (hereafter 11.5-0 kyr BP) is a significant period for studying the climate evolution and variability to improve our knowledge of the climate system. The period is well known and archived with proxy data (e.g., Masson et al., 1999; Bonfils

90   et al., 2004; Braconnot et al., 2007a, b; Wanner et al., 2008; Mauri et al 2015). It is also a period used to evaluate how climate models respond to the variations in insolation in response to astronomical forcing (Fischer and Jungclaus, 2011). In the early Holocene, the astronomical forcing was very different from today because of changes in three astronomical parameters (eccentricity, obliquity, and the precession) which alter the amount and distribution of incoming solar energy at the top of the atmosphere (Berger, 1978). According to Berger (1978), during the early Holocene at 11 kyr BP, the Northern Hemisphere

95   received about 30 W/m^2 more insolation during boreal summer than at present, which caused the climate to be relatively warm during the early to mid-Holocene. This relatively high summer insolation resulted in the reorganization of various variables of the climate system, such as the melting of the ice sheets (including the Fennoscandia Ice Sheet, FIS and Laurentide Ice Sheet, LIS), and the associated freshwater release in different regions during the early Holocene (Briner et al., 2016; Zhang et al., 2016).

100

Previous climate model studies, when compared to proxy data for the mid Holocene, suggest that most climate models were able to simulate the cooler and wetter climate of Southern Europe (e.g., Brewer et al., 2007; Brayshaw et al., 2011). However, some models find it difficult to simulate the magnitude of the climate patterns as seen in the reconstructed pollen data (Masson et al., 1999; Bonfils et al., 2004; Brewer et al., 2007). For instance, compared to proxy-based reconstructions, most models

105 simulate cooler and wetter climate in Southern Europe (Brewer et al., 2007), and wetter conditions in the Mediterranean regions during the early Holocene (Brayshaw et al., 2011).

Within this study, we present a simulation of the transient Holocene climate evolution during the last 11.5-0 kyr BP in Europe, performed with both the standard version of the iLOVECLIM model (Roche et al., 2014) and a version with dynamical

110 downscaling (Quiquet et al., 2018). We have increased the spatial resolution in Europe from (5.6° latitude × 5.6° longitude) to (0.25° latitude × 0.25° longitude). Our general objective is to examine the impact of the dynamical downscaling on the model results and evaluate if the model (with dynamical downscaling) simulates the climate during the Holocene in better agreement with proxy-based reconstructions. Thus, our main goal is to evaluate the benefits of using dynamical downscaling in paleo-climate simulation. In addition, we will assess the impact of the model resolution on their sensitivity at high spatial resolution.

115 We wish to provide a comprehensive and consistent overview of the climate system at a fine resolution during the Holocene. We will answer the following questions in this paper:

(i)   What is the impact of dynamical downscaling on the precipitation patterns during the Holocene in different, Regions in Europe?

(ii)   Do the high-resolution results of precipitation in the mountainous regions (e.g., the Alps, the Scandes and the

120   Scottish Highlands) produce Holocene climate patterns that compare more favorably to proxy data when compared with the low-resolution results?

(iii)   What is the advantage of using cheap numerically dynamical downscaling for paleoclimate research?
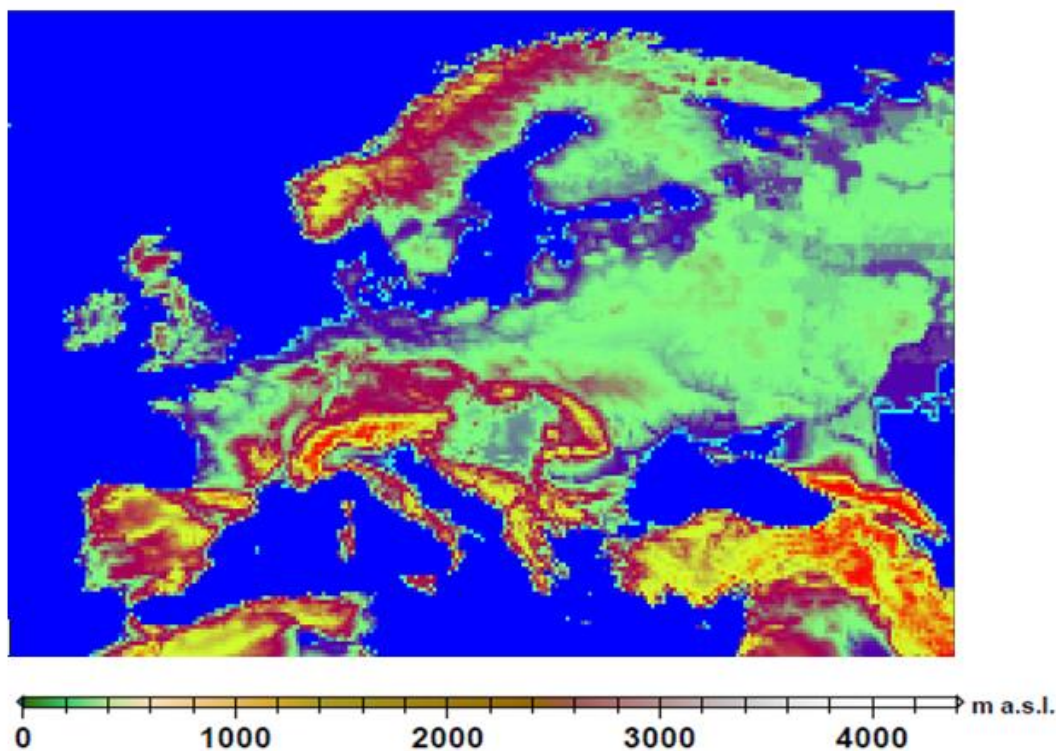
125

Fig 1. The extend of the Europe Grid (Plot of Topography) - sub-grid used for the downscaling

2.0 Methods (Model and Simulations)

2.1.1 The ILOVECLIM Model

130   iLOVECLIM (hereafter version 1.0) (Roche et al., 2014) is a three-dimensional model, with a simplified representation of the atmosphere relative to GCMs. This simplification and its lower spatial resolution make iLOVECLIM much faster than coupled GCMs (Goosse et al., 2010; Kitover et al., 2015). It is a fork of the LOVECLIM 1.2 model code (Goosse et al., 2010), and it has the main climate system components in common. We apply here a version that includes the following components: the atmospheric model, ECBilt (Opsteegh et al., 1998), the sea-ice ocean component, CLIO (Goosse and Fichefet, 1999), and the

135   terrestrial vegetation model, VECODE (Brovkin et al., 1997).

Our model version is a direct follow-up of the ECBilt-CLIO-VECODE coupled climate model and has been successfully used to simulate some key past and future climates, for example the Last Glacial Maximum (e.g., Timmermann et al., 2004; Roche et al., 2007), the last deglaciation (e.g., Timm et al., 2008), the Holocene (e.g., Renssen et al., 2005a, b), the last millennium

140 (e.g., Goosse et al., 2005a, b) and the 21st Century (e.g., Schaeffer et al., 2002, 2004; Driesschaert et al., 2007). The atmospheric component (ECBilt) includes three vertical levels at 800, 500 and 200 hPa and applies the quasi-geostrophic potential vorticity equation to model the dynamical processes in the atmosphere (Opsteegh et al., 1998). It runs on a global spectral grid truncated at T21 that represents a horizontal resolution of 5.6° latitude and 5.6° longitude. Another component of the model, CLIO, Coupled Large-scale Ice-Ocean model (Goosse et al., 2010), is a three-dimensional free-surface Ocean General circulation

145 model which has been coupled with a full sea ice model (Goosse and Fichefet, 1999). It has a horizontal resolution of 3° by 3° lat-lon and 20 layers in the vertical. VECODE runs on the same grid as ECBilt and includes three different plant functional types (PFTs): trees, grass, and desert/bare soil, each with different physical properties for evapotranspiration, surface roughness and albedo. The vegetation fraction (v) is calculated by the sum of the tree fraction (f) and grass fraction (g) (Brovkin et al., 2002; Goosse et al., 2010).

150

2.1.2 Dynamical Downscaling

In this study, we apply the dynamical downscaling presented by Quiquet et al. (2018) for precipitation and temperature in the coupled iLOVECLIM model. The downscaling is done from the original ECBilt's T21 grid towards an European domain between 13.875° W and 49.875° E in longitude and 35.125° N and 71.875° N in latitude with a resolution of 0.25° in lat-lon.

155 The basic idea behind the dynamical downscaling process is to reproduce the model physics of ECBilt (not the dynamics) on a higher spatial resolution so that the sub-grid orography is explicitly considered. To do so, we use artificial vertical layers, so that variables such as temperature and precipitation formation can be computed at any altitude in the sub-grid orography for each atmospheric time step (Quiquet et al., 2018). We follow a conservative approach in which the "large scale" fields (on the native grid) are the sum/mean of what is computed on the sub-grid. The results from Quiquet et al. (2018) show that, in

160 comparison to the standard version of the model, the downscaling improves the vertical distribution of temperature (for example, with a more realistic profile in mountainous regions) and the precipitation distribution in mountainous regions. However, the results also suggest that dynamical downscaling is not able to correct the biases of the large-scale native model, which are mostly driven by the model's simplification and to the atmospheric circulation, which is not downscaled (Quiquet et al., 2018).

165

To apply dynamical downscaling in the model, the temperature and moisture variables on the vertically extended native (ECBilt) grid are recomputed in the model. The computation is done on the 11 vertical levels of the grid (10, 250, 500, 750, 1000, 1250, 1500, 2000, 3000, 4000 and 5000 m) (Quiquet et al., 2018), by using the equations required for the vertically

extended grid defined by Haarsma et al. (1997). The atmospheric boundary layer is not well represented in the ECBilt, hence
170 the heat and moisture fluxes at the earth surface are computed based on an idealized vertical profile (Quiquet et al., 2018). The
temperatures are computed based on hydrostatic equilibrium and the ideal gas law at the 650 and 350-hPa horizon, with the
assumption that the atmosphere is isothermal above 200 hPa. Above 500 hPa, the atmosphere is assumed dry (Goose et al.,
2010). The temperatures and precipitation at the sub-grid orography are then computed from the climate variables obtained or
computed from the vertically extended artificial grids (Quiquet et al., 2018). For detailed information, such as an explanation
175 of the physics applied on the dynamical downscaling in the model, the reader is referred to Quiquet et al. (2018).

2.1.3 Experimental set-up

We applied iLOVECLIM-1.0 (Roche et al., 2014) and iLOVECLIM-1.1 (Quiquet et al., 2018) to simulate the transient
evolution of the climate during the last 11.5 kyr (Table 1). Two experiments were performed (hereafter 11.5K_Standard and
180 11.5K_Down). The experiment 11.5K_Standard is performed with the standard version of the model on the low-resolution
T21 grid. The second experiment (11.5K_Down) is when dynamical downscaling has been applied to the quasi-geostrophic
T21 grid to compute the temperature and precipitation on the regional sub-grid in Europe (Fig. 1). We forced the simulations
with orbital forcings (Berger, 1978) and atmospheric trace gas concentrations of CO_2, CH_4 and N_2O (Raynaud et al., 2000)
which vary annually for the 11.5-0 Kyr BP simulation period. Constant ice sheet configurations were prescribed for the
185 experiments. while the solar constant and aerosol levels were kept fixed at pre-industrial levels. During the Holocene, the
astronomical forcing determines variations in terms of seasons and latitudes of the incoming solar radiation at the top of the
atmosphere. For example, at 65°N, the summer insolation is reduced by 30 W/m^2 throughout the Holocene epoch (Fig. 2). The
ice core-based levels of CO_2, CH_4 and N_2O represent 1 W/m^2 variability in radiative forcing (Schilt, 2010). This greenhouse
gas (GHG) forcing was at its maximum level at 10 Kyr BP and then started decreasing to a low value at 8 Kyr BP before rising
190 again during the last 6 Kyr BP to preindustrial values (Fig. 2). The experiments were initialized with a state derived from an
experiment that was run for 1000 years until equilibrium with 11.5 Kyr BP astronomical parameters, greenhouse gas levels,
and ice sheets.

We present the results of precipitation and temperatures as anomalies from the pre-industrial period of our experiments (1000-
195 250 yr BP) and compare the results of both 11.5K_Standard and 11.5K_Down.

200

Table 1: Summary of the main features of the model and experimental set-up

simulations		
Model	**ILOVECLIM (Standard Version)**	**iLOVECLIM (Dynamical downscaling)**
Component	Ocean, sea ice, atmosphere, vegetation	
Atmospheric Resolution (lat × lon)	5.6° × 5.6°	0.25° × 0.25°
Oceanic component Resolution	3° × 3°	
Prescribed forcings and reference	Orbital forcings Berger (1978) GHG Schilt et al., (2010) Raynaud et al., (2000) Icesheets, Fixed	
Initial condition	Equilibrium experiment at 11.5 ka (1kyr)	
Duration of experiment	11.5 kyr	

205

210
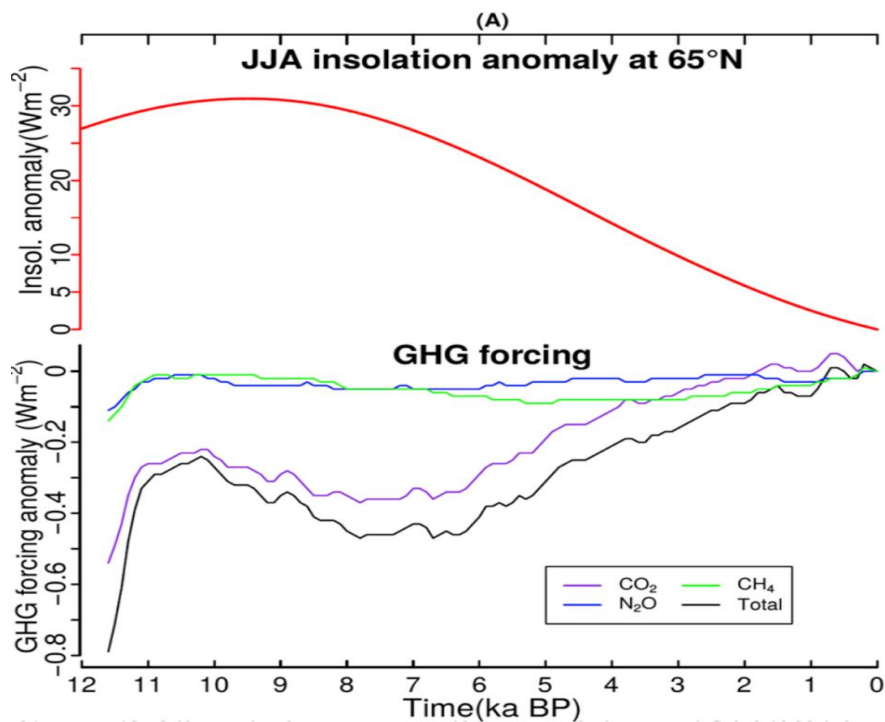
Fig 2. Climate forcings used in the experiment GHG forcings and summer June July August (JJA) insolation at 65° N (both in Wm^2) during the Holocene (Fig taken from; Zhang et al., 2018)

215

220

225

230

3.0 Results

3.1.1 Spatial distribution of temperature and precipitation in Europe

3.1.2 Temperature

Simulated temperatures of 11.5K_Down and 11.5K_Standard (Fig 3) show some similarities in terms of their pattern.
235 However, as expected more details are visible in 11.5K_Down than 11.5K_Standard. The downscaling produces local temperature changes, visible on the high-resolution grid (11.5K_Down) particularly in northern Scandinavia and the Alps at both 9 kyr BP and 6 kyr BP (Fig 3 d & e). Simulated temperature anomaly for 11.5K_Down and 11.5K_Standard was warm at both 9 kyr Bp and 6 kyr BP with a temperature anomaly (relative to pre-industrial) of up to 4 °C for 9 kyr BP and 2 °C for 6 kyr Bp. Central Europe and south-west Europe has a positive temperature anomaly relative to pre-industrial between 0.5-1
240 °C at 9 kyr BP. Only south Turkey has a negative temperature anomaly up to -2 °C at 9 kyr BP. During the mid-Holocene, northern Scandinavia was 2 °C warmer than pre-industrial. Northern Europe was warm with a temperature anomaly of 0.5 °C. The south-eastern corner of the domain was cool with a negative temperature anomaly of -1 °C at 6 kyr BP. At 3 kyr BP, most regions in Europe were cooler than pre-industrial except the south-western part which had a positive surface temperature anomaly of up to 0.5 °C. The latitudinal pattern during the mid-Holocene shows that it was warmer at the high latitudes than
245 the mid latitude. These spatial patterns in our results during the mid-Holocene appears to agree with PMIP2 related work analyzed by Brewer et al. (2007) who found cooler temperatures in the south and warmer temperatures in the north of Europe. Our model however simulates cooler conditions in south-eastern Europe but slightly higher temperatures in the south-west, which contradicts the cool conditions in the south-west suggested by Brewer et al. (2007). Reconstructions of mean annual temperature in the mid-Holocene by Wu et al. (2007) reveal a similar pattern in some regions to our results, showing intense
250 cooling in southern Europe and warming over northern and central Europe. However, our model simulates similar magnitude of warming over northern Scandinavia, which is more in agreement with Mauri et al. (2015).

Overall, it can be observed that in many regions for all time slices, the native grid (T21/11.5_Standard) is still seen on the 11.5K_Down model results. This is because the main impact of the dynamical downscaling is to compute physically the climate
255 variables which are connected to temperature in accordance to the sub grid topography for a given course-grid information.
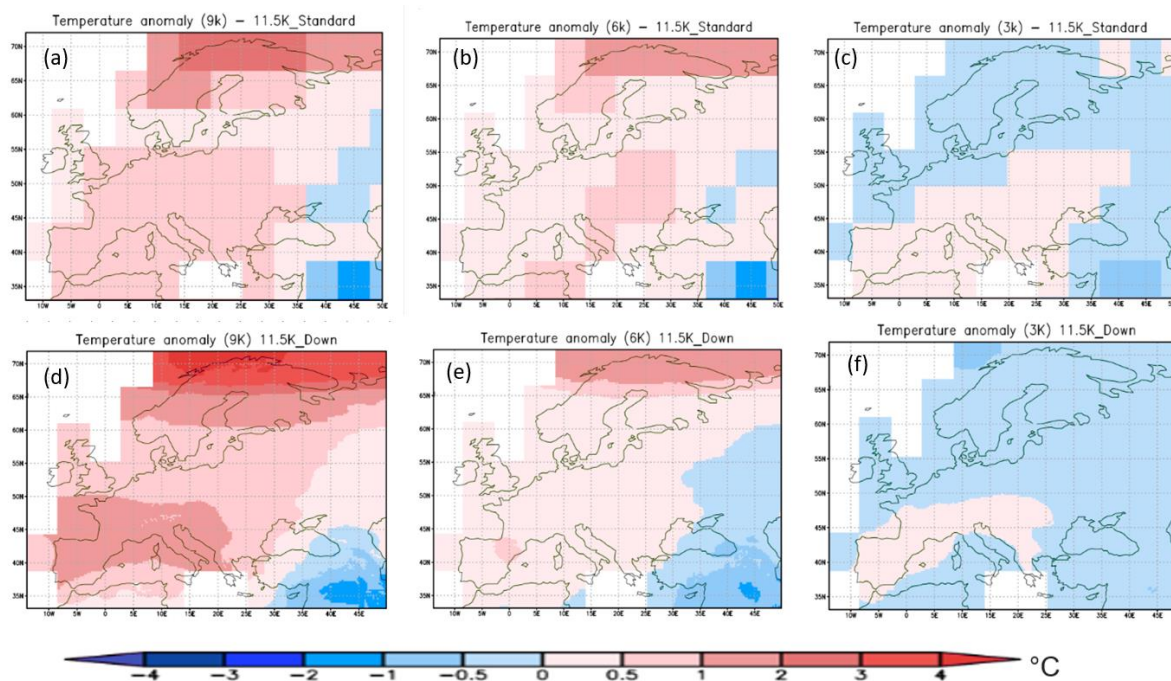
Fig. 3: Simulated temperature anomalies (°C) showing spatial distribution in Europe for 9 kyr BP (a & d), 6 kyr BP (b, e) and 3 kyr BP (c, f) for 11.5K_Standard and 11.5K_Down.

260

.

3.1.3 Precipitation

The simulated precipitation shows that 11.5K_Down provides more spatial detail than 11.5K_Standard, and better considers
265 the impact of topography on precipitation (Fig 4). This time as compared to the temperature results, the pattern for both simulations does not look the same. The results reveal that with 11.5K_Down we can drastically increase the spatial variability of the model in topographic regions when compared to the 11.5K_Standard. For instance, our 11.5K_Down experiment provides a more detailed view in the Scandes Mountains, the Alps, the Scottish Highlands and the Pyrenees. The Scandes mountains are characterized by wetter than pre-industrial conditions at 9 and 6 kyr BP for the 11.5K_Down, but relatively
270 drier conditions at 9, 6 and 3 kyr BP than pre-industrial for the 11.5K_Standard (Fig 4). The precipitation anomaly in the Scandes Mountains at 9 kyr BP was about 250 mm/yr for the 11.5K_Down, while the 11.5K_Standard has precipitation anomaly of -50 mm/yr. The precipitation anomaly in the mid Holocene (6 kyr BP) was up to 50 mm/yr and -50 mm/yr in Scandinavia for the 11.5K_Down and the 11.5K_Standard of the model respectively. In the Alps, the Pyrenees and the Massif Central, the 11.5K_Down simulated precipitation at 9 kyr BP was up to 150 mm/yr higher than pre-industrial, and this detailed
275 information is not seen in 11.5K_Standard (Fig 4). Even at 6 kyr BP, our 11.5K_Down precipitation provides additional

information in the Alps with precipitation anomaly up to 50 mm/yr. The Scottish Highlands show precipitation of about 350 mm/yr up to 400 mm/yr wetter than the pre-industrial in the early Holocene (9 kyr BP) for the 11.5K_Down. However, it was about 50 mm/yr drier than pre-industrial in the late Holocene (3 kyr BP) for both the 11.5K_Down and 11.5K_Standard experiments in the Scottish Highlands. The Scottish Highlands were still up to 100 mm/yr wetter in the mid-Holocene than

280   pre-industrial for 11.5K_Down; this was approximately 50% less in the 11.5K_Standard grid that shows precipitation anomalies between 50 mm/yr up to 100 mm/yr. The mountain ranges drastically affect the local precipitation anomalies, eventually changing the sign of the standard model (e.g., the downscaled Alps or the Scandes are most of the time in opposition with the standard model, that is. wetter becomes drier and drier becomes wetter. The higher precipitation anomaly in these mountainous regions for the high-resolution grid is due to the impact of the downscaling, as the primary effect of the

285   downscaling is to increase precipitation in elevated areas (e.g., the Scandes Mountains and the Alps). The results with dynamical downscaling provide details of the precipitation that better reflect the effect of the underlying topography. In general, experiment 11.5K_Down is relatively wetter than 11.5K_Standard in most topographically complex regions in Europe: because the downscaling scheme is more simply redistributing precipitation.

290   The simulated annual precipitation anomalies with respect to pre-industrial for the 11.5K_Down grid reproduce some of the major large-scale structures in Europe. For instance, the annual precipitation anomaly of the 11.5K_Down shows a pattern characterized by a relatively dry zone in central Europe, which splits wetter areas south and east of the Mediterranean (Morocco, Algeria, Turkey and Middle East) from wetter north-west Europe, especially at 9 kyr BP and 6 kyr BP (Fig 4). At 9 kyr BP, south-west Iberia and southern Turkey were wetter with a precipitation anomaly ranging from 100 mm/yr to 400

295   mm/yr. and showing more spatial details. This is generally true for 11.5K_Standard but the spatial details do not provide much information compared to the 11.5K_Down grid. North-west Europe has a precipitation anomaly of about 50 mm/yr to 300 mm/yr at 9 kyr BP. In contrast, the dry zone in central Europe is characterized by a precipitation anomaly of up to -50 mm/yr at 9 kyr BP. The impact of dynamical downscaling is seen in the results, as the downscaling reproduces some local topographical features in these regions. The results in the 11.5K_Down suggests that northern Italy was about 50 mm/yr drier

300   relative to the pre-industrial. However, compared to the 11.5K_Standard, northern Italy was relatively up to 50 mm/yr wetter than the pre-industrial. Other regions such as north-east Europe (especially western Russia) was generally dry (about -50 mm/yr) throughout the Holocene for the 11.5K_Down grid at 9 and 6 kyr BP but was relatively wet (up to 50 mm/yr) for 11.5K_Standard. The Iberian Peninsula in the 11.5K_Down grid was between 50 mm/yr and 100 mm/yr wetter than pre-industrial at 9 Kyr BP, but up to -50 mm/yr drier than pre-industrial for the simulated 11.5K_Standard.

305
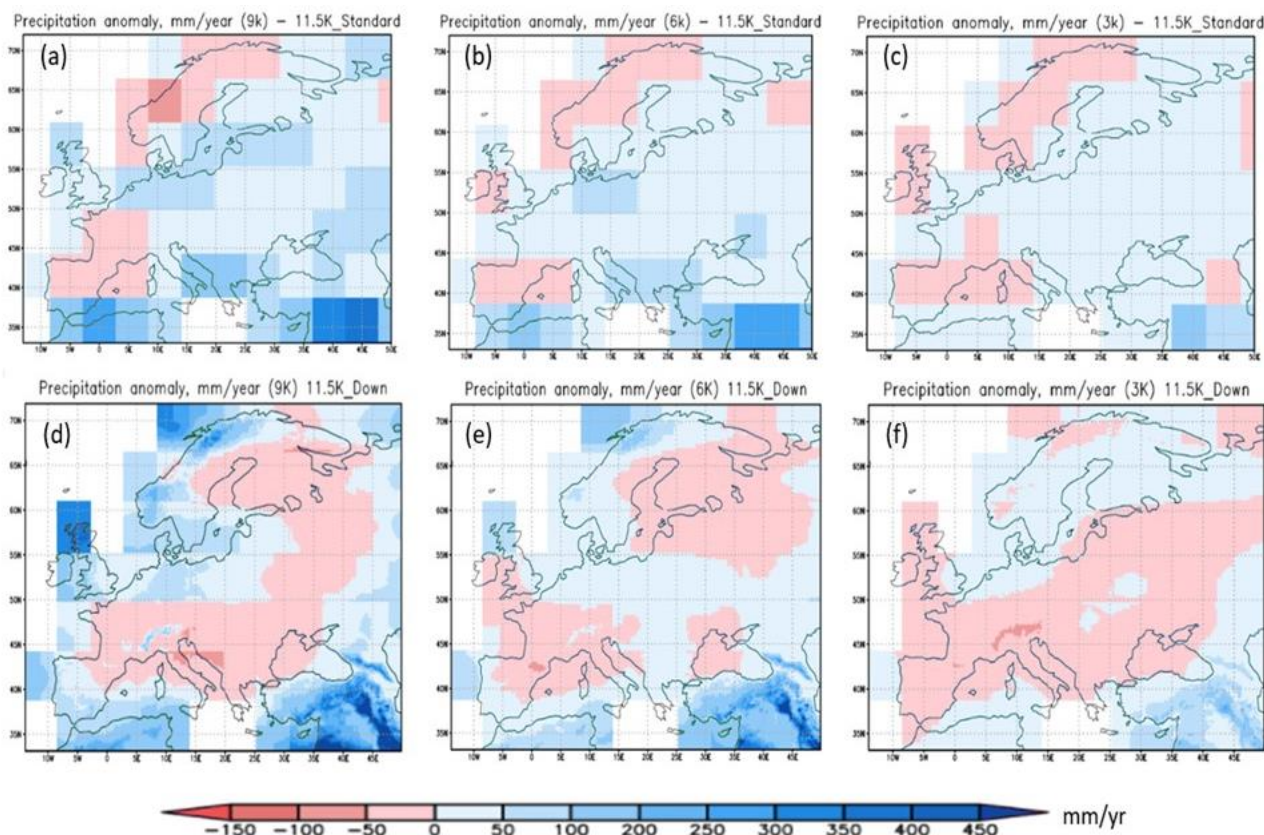
Fig. 4: Simulated precipitation anomalies (mm/yr) showing spatial distribution in Europe for 9 kyr BP (a & d), 6 kyr BP (b & e) and 3 kyr BP (c & f) for 11.5K_Standard and 11.5K_Down.

310

3.2 Temporal Trends in Annual Precipitation in Europe

In most areas, applying dynamical downscaling leads to an increase in precipitation compared to the standard experiment. The average precipitation in Europe for the entire Holocene was 775 mm/yr and 624 mm/yr for 11.5K_down and 11.5K_Standard respectively. Consequently, this shows about 24% increase in precipitation for the whole of Europe when downscaling is applied. In both experiments, it was generally wetter in the early and mid-Holocene than pre-industrial especially between 10 and 7 kyr BP. For the 11.5K_down model, precipitation generally rises from 762 mm/yr at 11 kyr BP to its maximum peak value of 822 mm/yr between 9 and 8.5 kyr BP, and slightly decreases after 7.5 kyr BP to 746 mm/yr in the late Holocene (Fig 5). This precipitation trend in the Holocene is similar to 11.5K_Standard. Precipitation was about 622 mm/yr at 11 kyr BP for the 11.5K_Standard, then rises steadily to 666 mm/yr between 9 and 8.5 kyr BP before declining gradually to 593 mm/yr

320   towards the preindustrial. The mid-Holocene was 32 mm/yr wetter than the pre-industrial in the 11.5K_down. The precipitation

has a decreasing trend until the Pre-industrial.
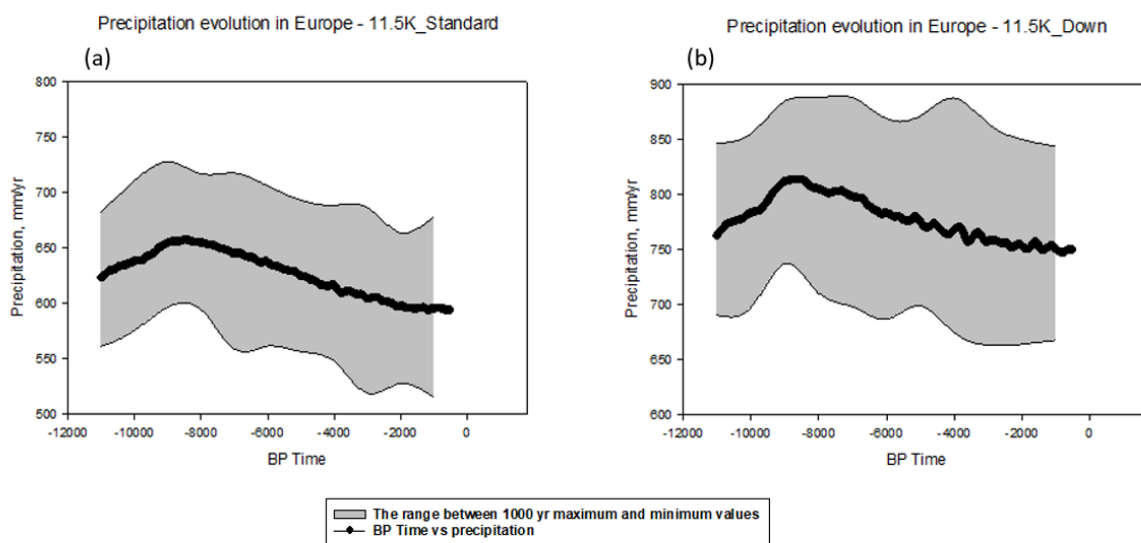
Fig. 5: Precipitation evolution in Europe during the Holocene for both 11.5K_Standard (Left) and 11.5K_Down (Right).

325

3.2.1 Regional Precipitation (Scandes Mountains, Alps, and Scottish Highlands)

One of our objectives in this study is to evaluate our model's performance for regions with elevated topography. We compare

the precipitation from reconstructed proxy data over the Alps, the Scandes Mountain, and the Scottish Highlands (latitude and

330   longitude in Table 2) with our model results.

Table 2: Latitude and Longitude information for the Regions of interest

Region	Longitude	Latitude
Scandes Mountain	15°E ~ 20°E	66.5°N ~ 70°N
Alps	5°E ~ 12°E	44°N ~ 48°N
Scottish Highland	6°W ~ 4°W	56°N ~ 58.5°N

335

Scandes Mountain

340   Compared to 11.5K_Standard, our 11.5K_Down produces about twice as much precipitation in the Scandes Mountains, with an opposite long-term trend. In the downscaled version, precipitation rises gradually from 1233 mm/yr at 11 kyr BP to its maximum peak of 1469 mm/yr around 9 kyr BP (Fig 6), after which precipitation started declining gradually to 1 kyr BP. This contrasts with the 11.5K_Standard, which has rising precipitation trend from 525 mm/yr at 11 kyr BP to the pre-industrial level of 637 mm/yr (Fig 6 a). In addition. there is a clear maximum peak at 9 kyr BP in the 11.5K_Down that is absent in the 11.5K_Standard.

345

Alps

350   Similar to the Scandes Mountain, there is a doubling of the precipitation in the 11.5K_down when compared to the 11.5K_Standard in the Alps. The trends for both experiments are similar with reduced precipitation in the early Holocene, and a more or less flat trend afterwards (Fig 6). The precipitation trend in the Alps for the 11.5K_Down shows that these mountains were drier in the early Holocene when compared to pre-industrial, with the late Holocene showing a flat trend towards the pre-industrial. Thus, there is higher precipitation in the late Holocene than the early Holocene for the 11.5K_Down. The figure for the 11.5K_Down shows a slight increase of precipitation in the early Holocene towards 7 kyr BP followed by a slight dip and

355   stable trend towards pre-industrial. For the 11.5K_Standard, the precipitation rises from 11 Kyr BP was quite steady and stable to the late Holocene with less variability when compared to the 11.5K_Down.

Scottish Highlands

360   In the Scottish Highlands, the 11.5K_Down model simulates the highest average precipitation in Europe with a Holocene mean value of 3238 mm/yr, compared to 1077 mm/yr for the 11.5K_Standard. This is about three times higher than the 11.5K_Standard. Generally, precipitation rises from 11.5 Kyr BP to its maximum peak average of 3474 mm/yr around 8.7 Kyr BP and declines gradually through the rest of the Holocene for the 11.5K_Down (Fig 6 f). Compared to pre-industrial, the 11.5K_Down simulates wetter conditions in the early and mid-Holocene, after 3.6 Kyr BP to 0 kyr BP, the model simulates a

365   stable trend. The precipitation pattern for the 11.5K_Standard is quite different from the 11.5K_Down. The 11.5K_Standard shows gradual decline towards pre-industrial while the decrease in the 11.5K_Down is more pronounced with its maximum peak at a different time.
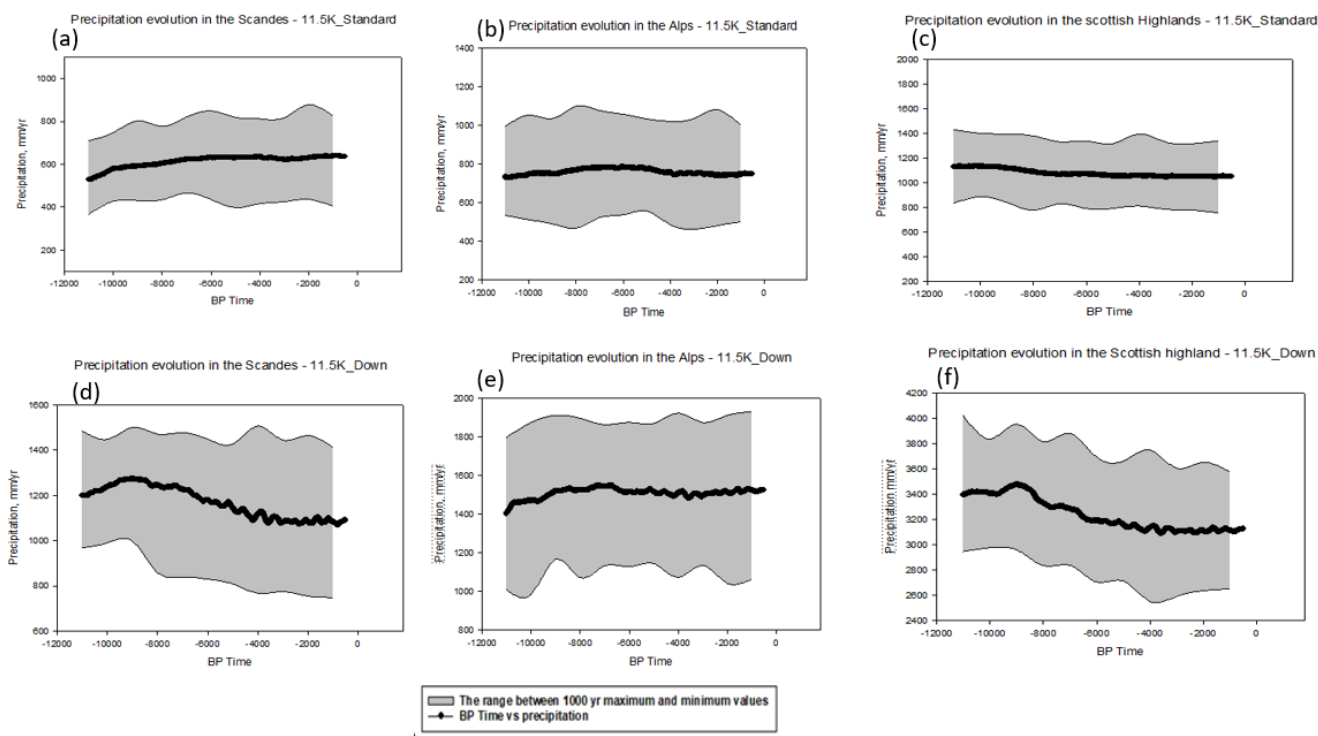
370

Fig. 6: Regional precipitation evolution in some mountainous regions in Europe for both the 11.5K_Standard and 11.5K_Down. Scandes Mountain (a & d), Alps (b & e), Scottish highland (c & f).

4.0 Discussion
375

The precipitation values simulated by 11.5K_Down clearly show the influence of topography, since the highest values of above 400 mm/yr are produced in mountainous regions such as Scandes, Scotland and the Alps, which has a much higher elevation. The basic effect of dynamical downscaling is to redistribute precipitation in a physically consistent way based on topography. (Quiquet et al., 2018). In most cases, 11.5K_Standard is wetter than 11.5K_Down in less elevated regions (Fig 4). For example,
380 some parts of central Europe are relatively dry in 11.5K_Down at 9 kyr BP but are relatively wet in 11.5K_Standard. Since the topography in 11.5K_Down is more realistic, the spatial pattern obtained and distribution with the downscaling is better than the standard version. Thus, downscaling reproduces local features of these mountain regions described in the results, with higher precipitation in agreement with what is known from modern observations. The annual and selected regional precipitation trends presented in the results reveal that all the selected regions in the 11.5K_Standard experiment present less
385 precipitation. In comparison, 11.5K_Down simulates much higher precipitation, coinciding with topography variations.

4.1.1 Data – Model comparison (performance of the dynamical downscaling)

Our 11.5K_Down simulation represents climate at a regional scale closer to the spatial scale of proxy data than our 11.5K_Standard experiment. The improvement resulting from the downscaling technique will impact the comparison of our
390 results with other climate model simulations and proxy-based reconstructions, especially because the latter are influenced by local conditions that are more realistically represented in the model. Previous model-data comparisons have revealed that General Circulation Models (GCMs) have great difficulty simulating key Holocene climate features, particularly trends in southern Europe (Mauri et al., 2014). One important factor could be the coarse resolution of GCMs (about 200-600km) relative to the regional and local climate represented by proxy records. Thus, these models may not be able to account for a fine-scale
395 variability of local features such as complex topographies. To evaluate the performance of our model, we have compared our 11.5K_Down and 11.5K_Standard precipitation results for some regions in Europe with available proxy data and other simulated climate models.

We assess the performance of our simulations in the Alps with a proxy-data reconstructions based on pollen data from the
400 Italian Alps (Furlanetto et al., 2018). The level of mid-Holocene precipitation reconstructed by Furlanetto et al. (2018) for the Italian Alps is between 1300 and 1700 mm/yr, which is in close agreement with our 11.5K_Down simulation that suggests precipitation between 1400-1500 mm/yr. Their reconstruction thus suggests that precipitation in the Alps was much higher than the 750 mm/yr suggested by 11.5K_Standard and supports the higher values that can be seen in the Alps for our 11.5K_Down simulations and confirming that the 11.5K_Standard is less realistic than the 11.5K_Down. The 11.5K_Standard
405 result of 750 mm/yr is more appropriate for precipitation of the surrounding lowlands, which would be expected as the standard experiment does not take into consideration the topography in the Alps. The trend for their reconstruction Furlanetto et al. (2018) is similar to Mauri et al. (2015), which reconstructs an increase in precipitation from early to mid-Holocene, while our 11.5K_Down experiment do not show such a significant trend of increase although the magnitude of precipitation is in high agreement. However, in terms of the precipitation temporal trend our 11.5K_Down agrees with lake-level reconstructions by
410 Harrison et al. (1996) that suggest no clear Holocene trend in lake-level records derived from some high-altitude sites (above 1000 m) in the Alps such as (Landos and Rousses). In summary, these previous proxy-based studies from the Alps confirm that our downscaled simulated 11.5K_Down provides a much better representation of Holocene precipitation of this mountain range than the 11.5K_Standard simulation without downscaling.

415 Comparing our 11.5K_Down with the 11.5K_Standard version of our simulations for the Scandes Mountains, 11.5K_Down shows that the early Holocene (10 -5 kyr BP) is a wetter period which is followed by drier conditions in the late Holocene, while the 11.5K_Standard result is characterized by flat precipitation pattern with no significant trend (Fig 6). Similar to the Alps, proxy data support our result with downscaling, as proxy-based precipitation reconstructions from Scandinavia suggest

a more humid and wet early Holocene, followed by a dry mid to late Holocene (Seppä and Birks, 2001; Bjune et al., 2004;

420   Harrison et al., 1996). For example, the pollen-based climate reconstructions by Seppä and Birks (2001) has in Scandinavia a similar trend as our 11.5K_Down result, showing enhanced precipitation in the early Holocene, which decreased steadily towards the late Holocene. This pattern is not seen in the 11.5K_Standard simulations. Bjune et al, (2005) reconstructed winter precipitation based on Holocene glacier behavior and show drier conditions in Scandinavia from 11.5 to 8 kyr BP, a wetter period from 8 to 4 kyr BP, followed by a drier period after 4 kyr BP to pre-industrial. The pattern of their results thus concurs

425   with our 11.5K_Down simulation (Fig 6). Moreover, pollen-inferred precipitation anomalies from Mauri et al. (2015) show that the spatial pattern in their precipitation at the Scandes Mountains is similar to our downscaling experiment presented in Fig 4. Consequently, our 11.5K_Down results is in better agreement with the proxy-based reconstructions than our 11.5K_Standard in most available studies, confirming that downscaling also provides a more realistic representation of the hydroclimate in Scandinavia.

430

The comparison with proxy-based reconstructions in our third region, the Scottish Highlands, is hampered by the unavailability of suitable records. However, a comparison to modern data makes clear that our dynamical downscaling results are much more representative of the precipitation in the high-altitude Scottish Highlands than the standard results. Our precipitation values in this region for the high resolution was overestimated by the model, but we can have some confidence that 11.5K_Down

435   represents the Holocene precipitation conditions also better than 11.5K_Standard. due to the spatial variability.

We also compared our 11.5K_Down results with studies in the Mediterranean. This region is very sensitive to changes in humidity, and during the early and mid-Holocene period, the dominant controlling factor on the Mediterranean ecosystem was precipitation rather than temperature (Magny et al., 2013; Mauri et al., 2015; Peyron et al., 2011). There are some proxy-based

440   reconstructions and climate model simulations in the Mediterranean region that can be compared to our study. For instance, Brayshaw et al. (2011) used the HadSM3 global climate model, which was downscaled to about 50 km using a regional climate model (HadRM3), to simulate enhanced precipitation for the entire Holocene in the Mediterranean. This is consistent with the results of our 11.5K_Down high-resolution model, which simulates wetter conditions during most of the Holocene relative to pre-industrial (Fig 4). Their regional climate model simulations show that some coastal areas particularly in the north-eastern

445   Mediterranean received more precipitation at 9 kyr BP and 6 kyr BP (Brayshaw et al., 2011). This agrees with our high-resolution model that simulates higher precipitation above 450 mm/yr around the Balkans and Southern Turkey.

Our 11.5K_Down result show also a contrasting pattern between regions in the Mediterranean, the southern and eastern Mediterranean being wet and the western-central part being dry (Fig. 4), particularly during the early-to-mid Holocene. This

450   pattern is similar to reconstructions based on proxy data, such as lake levels, pollen data, and stable isotopes. All these data show that throughout the Holocene, climate conditions in the Mediterranean region varied spatially and temporally (e.g., Mauri

et al., 2015; Sadori et al., 2016; Cheddadi and Khater, 2015). For instance, an east–west division during the Holocene is also observed in the Mediterranean region from lake-level reconstructions (Magny et al., 2013), marine and terrestrial pollen records (Guiot and Kaniewski, 2015) and speleothem isotopes (Roberts et al., 2011). Specifically, the simulated wetter mid-

455 Holocene conditions in 11.5K_Down agrees with the high precipitation reconstructed at 6 kyr BP (Bartlein et al. 2011; Guiot and Kaniewski, 2015; Mauri et al., 2015; Kuhnt et al., 2008). In the Mid-Holocene (6 kyr BP), precipitation values of (100-500 mm/yr) higher than pre-industrial levels was reconstructed in the Mediterranean by Bartlein et al. (2011), in agreement with our high-resolution simulation (Fig 4). Pollen-based reconstructions by Peyron et al. (2017) suggest dry early to mid-Holocene conditions in northern Italy like our dynamical downscaling simulations. The synthetic multi-proxy reconstruction

460 of Finne et al. (2019) for the Holocene in the Mediterranean shows a longer period of wetter conditions in the east and south as compared to the north and central areas of the Mediterranean. This was especially clear before 8.7 kyr BP. Their study also reveals that the driest period in the eastern Mediterranean was at 3 kyr BP, while Italy remained wetter around this time (Finne et al., 2019). Comparing their work with our 11.5K_Down, we can see some similarities. For instance, at 3 kyr BP, the eastern Mediterranean was the driest compared to the early Holocene and mid-Holocene. Our drier conditions simulated by

465 11.5K_Down at 3 kyr BP agrees with the reconstruction from their study.

As shown above, we can compare our high-resolution results with paleo-reconstructions in these complex mountainous terrain in Europe due to the spatial variability attained from the downscaling. Compared to other studies, we find that our downscaled precipitation simulations are consistently in line with some regions in Europe. Europe experienced multiple climate changes

470 of various magnitudes over the Holocene, and regions within experienced those changes differently. Based on our results, we can reproduce the different regional responses presented by proxy-based reconstructions, for instance in northern and southern Europe we find wetter conditions from the early to mid-Holocene relative to pre-industrial (Fig. 4), similar to the proxy-based reconstructions reported by (Mauri et al., 2015).

475 From a review of the Paleoclimate Modeling Intercomparison Project (PMIP2) by Braconnot et al. (2007) in the mid-Holocene, we can infer from their work that southern Europe was wetter and cooler. In addition, the eastern Mediterranean was characterized by high precipitation; eastern Europe including large portion of Russia, was wetter at the mid-Holocene than pre-industrial. In contrast, northern part of Europe was relatively dry. When comparing the 11.5K_Down simulations to Braconnot et al., (2007), we find that our results agree with some regions as well as in contrast with some other regions. For

480 instance, at 6 kyr BP, our model simulates wetter conditions in the eastern Mediterranean and a bit drier in northern Europe, which agrees with the results of Braconnot et al. (2007). However, our model simulates drier conditions in the eastern part of Europe towards Russia, which is in contradiction with the work of PMIP2.

4.1.2 What is the advantage of using dynamical downscaling for paleoclimate research?

485   The high-resolution in our simulations is clearly visible in the change pattern for precipitation events in the Holocene. In terms
       of climate impact studies, the local scale information achieved from downscaling can be very useful. With our high-resolution
       simulations, only the physical part of precipitation is downscaled. The main reason for precipitation increases over the
       mountains with the downscaling is simply because it is colder at high elevation and cold air cannot contain much humidity, so
       it rains out. But since we see more of the topography, it is better represented in the model. High-resolution climate modeling

490   can be very useful to paleoclimatologists for data comparison at the local scale. For example, if a scientist studying
       paleoclimate data retrieves data from high-elevated region such as the Alps or the Scandes Mountains, then it would be highly
       useful to get information on the gradients in precipitation and temperature provided by a high-resolution (regional) climate
       model. It is probable that these regional data have been impacted by these gradients, hence it can be expected that the spatial
       scale of the high-resolution (regional) climate model be in better agreement with the data than the course (global) resolution

495   model.

5.0 Conclusion

       In this study, we have applied dynamical downscaling to our low-resolution iLOVECLIM model in Europe, increasing its
       resolution from 5.56° to 0.25° latitude-longitude. To our knowledge, this is the first-time dynamical downscaling has been

500   applied for Holocene transient experiments. A transient simulation for the entire Holocene (11.5 – 0 kyr BP) was done for both
       the standard version of the model and with dynamical downscaling being applied. We have answered the following research
       questions in this paper:

       What is the impact of dynamical downscaling on the precipitation patterns during the Holocene in different complex regions

505   *in Europe?* We have compared the spatial and temporal annual precipitation results of the low-resolution grid with the high-
       resolution grid to analyze the impact of dynamical downscaling on the model. Our results suggests that when downscaling is
       applied for precipitation, it drastically increases the spatial variability particularly in the high-elevated regions as compared to
       the coarse resolution of the standard model.

510   *Are the high-resolution results of precipitation in the mountainous regions (e.g., the Alps, the Scandes Mountains and the*
       Scottish Highlands) producing more realistic Holocene climate when compared with the low-resolution grid and other proxy
       data? We have shown that the high-resolution simulation presents a better agreement with proxy-based reconstructions and
       other climate model studies as compared to the course (low) resolution grid particularly in the Mediterranean and mountainous
       regions in Europe. The downscaling scheme simulates much higher (by at least a factor of two) precipitation maxima and

515   provides detailed information in the Scandes Mountains, the Alps and the Scottish Highlands. By comparing our 11.5K_Down

and 11.5K_Standard with published proxy-based reconstructions, we can confirm that our 11.5K_Down simulates in some cases the right magnitude of the precipitation changes reconstructed by other proxy studies (For example in the Alps), and that there is good agreement for the overall trend and spatial pattern than the 11.5K_Standard. The different patterns of change such as wetter condition in northern and southern Europe as well as wetter conditions in the Mediterranean are well captured by our 11.5K_Down model. Overall, precipitation was higher during the early Holocene than the late Holocene in most regions in Europe when compared to the pre-industrial.

What is the advantage of using a numerically cheap dynamical downscaling in paleoclimate research? Paleoclimatologists would like to have very high-resolution model runs covering the last million years or more. We have shown a numerically cheap tool which is able to perform kilometric-multi-millennial simulations, even with a low resolution and a simple downscaling scheme, we achieve relatively good model-data agreement. The downscaling technique is moderate and, makes it appropriate for long-term integration and can hypothetically be applied and extended in further studies to any grid higher than the T21 grid. Our dynamical downscaling produces more detailed precipitation information suitable for comparison with regional paleoclimate studies. In addition, the downscaling simulation is better suited to match proxy data in terms of spatial representation, making them a useful platform for comparisons between climate models and proxy data. The dynamical downscaling's improved ability to resolve complex topography areas is very important since proxy records are often obtained from high altitudes, where the most sensitive climate archives (such as trees, corals, sediments and ice cores) are deposited.

Acknowledgement

The research is financed through the European Union's Horizon 2020 research and innovation programme within the TERRANOVA project, No 813904. The paper reflects the views only of the authors, and the European Union cannot be held responsible for any use which may be made of the information contained therein. Thanks to Marie Jose Gaillard who provided us with her input in setting up this work. Another thanks to Heikki Seppa and Basil Davis, who assisted us with proxy-based reconstructions.

Code Availability

The iLOVECLIM source code is accessible at http://www.elic.ucl.ac.be/modx/elic/index.php?id=289 (UCL, 2021). The developments on the iLOVECLIM source code are hosted at http: //forge.ipsl.jussieu.fr/ludus (IPSL, 2021), due to copyright restrictions they cannot be publicly accessed. Request for access can be made by contacting D. M. Roche (didier.roche@lsce.ipsl.fr). For this study, we used the model at revision 1147.

Data Availability

https://doi.org/10.23642/usn.19354082

Author contribution

The study was designed by all authors. AF performed the simulations and wrote the manuscript with contributions of HR, RF, DMR and AQ. The model results were analysed and interpreted by all authors.

Competing interests

None

References

Bartlein, P. J., Harrison, S. P., Brewer, S., Connor, S., Davis, B. A. S., Gajewski, K., Guiot, J., Harrison-Prentice, T.I., Henderson, A., Peyron, O., Prentice, I .C., Scholze, M., Seppä, H., Shuman, B., Sugita, S., Thompson, R. S., Viau, A. E,Williams, J., and Wu, H.: Pollen-based continental climate reconstructions at 6 and 21 ka: a global synthesis, Clim. Dynam., 37, 775–802, 2011.

Berger, A. L.: Long-term variations of daily insolation and Quaternary climatic changes, J. Atmos. Sci., 35, 2363–2367, 1978.

Bjune, A. E., Bakke, J., Nesje, A., and Birks, H. J. B.: Holocene mean July temperature and winter precipitation in western Norvay inferred from palynological and glaciological lake-sediment proxies. The Holocene, 15(2), 177–189. https://doi.org/10.1191/0959683605hl798rp, 2005.

Bonfils, C., de Noblet, N., Guiot, J., and Bartlein, P.: Some Mechanisms of mid-Holocene climate change in Europe, inferred from comparing PMIP models to data, Clim. Dynam., 23, 79–98, 2004.

Braconnot, P., Otto-Bliesner, B., Harrison, S., Joussaume, S., Peterchmitt, J.-Y., Abe-Ouchi, A., Crucifix, M., Driesschaert, E., Fichefet, Th., Hewitt, C. D., Kageyama, M., Kitoh, A., Laîné, A., Loutre, M.-F., Marti, O., Merkel, U., Ramstein, G., Valdes, P., Weber, S. L., Yu, Y., and Zhao, Y.: Results of PMIP2 coupled simulations of the Mid-Holocene and Last Glacial Maximum – Part 1: experiments and large-scale features, Clim. Past, 3, 261–277, doi: 10.5194/cp-3-261, 2007a.

Braconnot, P., Otto-Bliesner, B., Harrison, S., Joussaume, S., Peterchmitt, J.-Y., Abe-Ouchi, A., Crucifix, M., Driesschaert, E., Fichefet, Th., Hewitt, C. D., Kageyama, M., Kitoh, A., Loutre, M.-F., Marti, O., Merkel, U., Ramstein, G., Valdes, P., Weber, L., Yu, Y., and Zhao, Y.: Results of PMIP2 coupled simulations of the Mid-Holocene and Last Glacial Maximum –

Part 2: feedbacks with emphasis on the location of the ITCZ and mid- and high latitudes heat budget, Clim. Past, 3, 279–296, doi: 10.5194/cp-3-279, 2007b.

Brayshaw, D. J., Rambeau, C. M. C., and Smith, S. J.: Changes in the Mediterranean climate during the Holocene: insights
585   from global and regional climate modelling, The Holocene, 21, 15–31, 2011.

Brewer, S., Guiot, J., and Torre, F.: Mid-Holocene climate change in Europe: a datamodel comparison. Clim. Past. 3, 499e512., 2007.

590   Briner, J. P., McKay, N. P., Axford, Y., Bennike, O., Bradley, R. S., de Vernal, A., Fisher, D., Francus, P., Fr_echette, B., Gajewski, K., Jennings, A., Kaufman, D. S., Miller, G., Rouston, C., and Wagner, B.: Holocene climate change in Arctic Canada and Greenland. Quat. Sci. Rev. 147, 340e364, 2016.

Brovkin, V., Ganapolski, A., and Svirezhev, Y.: A continuous climate-vegetation classification for use in climate- biosphere studies. Ecol. Modell., 101, 251-261, 1997.
595

Castro, C. L., Pielke Sr., R. A., and Leoncini, G.: Dynamical downscaling: Assessment of value retained and added using the Regional Atmospheric Modeling System (RAMS), *J. Geophys. Res.*, 110, D05108, doi:10.1029/2004JD004721, 2005.

Cheddadi, R., and Khater, C.: Climate change since the last glacial period in Lebanon and the persistence of Mediterranean
600   species. Quaternary Science Reviews. 150. 146-157. 10.1016/j.quascirev.2016.08.010, 2016.

Claussen, M., Mysak, L. A., Weaver, A. J., Crucifix, M., Fichefet, T., Loutre, M.-F., Weber, S. L., Alcamo, J., Alexeev, V. A., Berger, A., Calov, R., Ganopolski, A., Goosse, H., Lohmann, G., Lunkeit, F., Mokhov, I. I., Petoukhov, V., Stone, P., and Wang, Z.: Earth system models of intermediate complexity: closing the gap in the spectrum of climate system models, Clim. Dynam., 18, 579–586, 2002.
605

Crowley T. J.: Causes of climate change over the past 1000 years. *Science (New York, N.Y.)*, *289*(5477), 270–277. https://doi.org/10.1126/science.289.5477.270, 2000.

Driesschaert, E., Fichefet, T., Goosse, H., Huybrechts, P., Janssens, I., Mouchet, A., Munhoven, G., Brovkin, V., and Weber,
610   S. L.: Modelling the influence of the Greenland ice sheet melting on the Atlantic meridional overturning circulation during the next millennia, Geophys. Res. Lett., 34, L10707, doi: 10.1029/2007GL029516, 2007.

Fallah, B., Sahar, S., and Ulrich, C.: Westerly jet stream and past millennium climate change in Arid Central Asia simulated by COSMO-CLM model, Theor. Appl. Climatol. 124, 1079–1088, 2016.

615

Feser, F., Rocker, B., von Storch, H., Winterfeldt, J., and Zahn, M.: Regional Climate Models add Value to Global Model Data: A Review and Selected Examples, B. Am. Meteorol. Soc., 92, 1181– 1192, 2011.

Finné, M., Woodbridge, J., Labuhn, I., and Roberts, C. N.: Holocene hydro-climatic variability in the Mediterranean: A

620   synthetic multi-proxy reconstruction. The Holocene, 29(5), 847–863. https://doi.org/10.1177/0959683619826634, 2019.

Fischer, N. and Jungclaus, J. H.: Evolution of the seasonal temperature cycle in a transient Holocene simulation: orbital forcing and sea-ice, Clim. Past, 7, 1139–1148, doi: 10.5194/cp-7-1139, 2011.

625   Furlanetto, G., Ravazzi, C., Pini, R., Vallè, F., Brunetti, M., Comolli, R., Novellino, M. D., Garozzo, L., and Maggi, V.: Holocene vegetation history and quantitative climate reconstructions in a high-elevation oceanic district of the Italian Alps. Evidence for a middle to late Holocene precipitation increase. Quat. Sci.Rev. 200, 212–236, 2018.

Gómez-Navarro, J. J., Montávez, J. P., Jerez, S., Jiménez-Guerrero, P., Lorente-Plazas, R., González-Rouco, J. F., and Zorita,

630   E.: A regional climate simulation over the Iberian Peninsula for the last millennium, Clim. Past, 7, 451–472, https://doi.org/10.5194/cp-7-451-2011, 2011.

Goosse H, and Fichefet T.: Importance of ice-ocean interactions for the global ocean circulation: a model study. J Geophys Res 104:23337–23355, 1999.

635

Goosse, H., and Fichefet, T.: The spatial and temporal complexity of the Holocene thermal maximum, Nat. Geosci., 2, 411– 414, doi:10.1038/ngeo513, 2009.

Goosse, H., Brovkin, V., Fichefet, T., Haarsma, R., Huybrechts, P., Jongma, J., Mouchet, A., Selten, F., Barriat, P.-Y., Campin, J.- M., Deleersnijder, E., Driesschaert, E., Goelzer, H., Janssens, I., Loutre, M.-F., Morales Maqueda, M. A., Opsteegh, T.,

640   Mathieu, P.-P., Munhoven, G., Pettersson, E. J., Renssen, H., Roche, D. M., Schaeffer, M., Tartinville, B., Timmermann, A., and Weber, S. L.: Description of the Earth system model of intermediate complexity LOVECLIM version 1.2, Geosci. Model Dev., 3, 603–633, https://doi.org/10.5194/gmd-3-603, 2010.

Goosse, H., Crowley, T., Zorita, E., Ammann, C., Renssen, H., and Driesschaert, E.: Modelling the climate of the last millennium: What causes the differences between simulations? Geophysical Research Letters, 32, doi 10.1029/2005GL22368,
645 L06710, 2005a.

Goosse, H., Renssen, H., Timmermann, A., and Bradley, R.S.: Internal and forced climate variability during the last millennium: a model-data comparison using ensemble simulations. Quaternary Science Reviews, 24, 1345-1360, 2005b.

Guiot, J. and Kaniewski, D.: The Mediterranean Basin and Southern Europe in a warmer world: what can we learn from the past? Front. Earth Sci., 3, 28, doi:10.3389/feart.2015.00028, 2015.

650

Haarsma, R. J., Selten, F. M., Opsteegh, J. D., Lenterink, G., and Liu, Q.: ECBILT: A coupled atmosphere ocean sea-ice model for climate predictability studies, KNMI technical report TR-195, De Bilt, The Netherlands, available at: http://bibliotheek.knmi. nl/knmipubTR/TR195.pdf (last access: January 2020), 1997.

655 Harrison, S. P., Yu, G., and Tarasov, P.: Late Quaternary lake-level record from northern Eurasia. Quaternary Research 45, 138–159, 1996.

Jacob, D., Bärring, L., Christensen, O. B., Christensen, J. H., de Castro, M., Déqué, M., Giorgi, F., Hagemann, S., Hirschi, M., Jones, R., Kjellström, E., Lenderink, G., Rockel, B., Sánchez, E., Schär, C., Seneviratne, S. I., Somot, S.,
660 van Ulden, A. and van den Hurk, B.: An inter-comparison of regional climate models for Europe: model performance in present-dayclimate. *Climatic Change*, 81, 31-52, http://dx.doi.org/10.1007/s10584-006-9213-4, 2007.
.
Jacob, D., Petersen, J., Eggert, B., Alias, A., Christensen, O. B., Bouwer, L. M., Braun, A., Colette, A., Déqué, M., Georgievski, G., Georgopoulou, E., Gobiet, A., Menut, L., Nikulin, G., Haensler, A., Hempelmann, N., Jones, C., Keuler, K., Kovats, S.,
665 and Yiuou, P.: EURO-CORDEX: new high-resolution climate change projections for European impact research. Regional Environmental Change, 14(2), 563-578. https://doi.org/10.1007/s10113-013-0499-2, 2014.

Jones, P., Osborn, T., and Briffa, K.: The evolution of climate over the last millennium, Science, 292, 662–667, 2001.

670 Kitover, D. C., van Balen, R., Roche, D. M., Vandenberghe, J., and Renssen, H.: Advancement toward coupling of the VAMPER permafrost model within the Earth system model iLOVECLIM (version 1.0): description and validation, Geosci. Model Dev., 8, 1445–1460, https://doi.org/10.5194/gmd-8-1445, 2015.

Kuhnt, T., Schmiedl, G., Ehrmann, W., Hamann, Y., and Andersen, N.: Stable isotopic composition of Holocene benthic
675 foraminifers from the Eastern Mediterranean Sea: Past changes in productivity and deep water oxygenation. Palaeogeography,
Palaeoclimatology, 2008.

Liu, Z., Otto-Bliesner, B., and Clark, P.: Synthesis of transient climate evolution of the last 21 ka (SynTRaCE-21) workshop.
PAGES News 19, 79e80, 2011.
680
Ludwig, P., Gómez-Navarro, J. J., Pinto, J. G., Raible, C. C., Wagner, S., and Zorita, E.: Perspectives of regional paleoclimate
modeling. Annals of the New York Academy of Sciences, 1436(1), 54–69. https://doi.org/10.1111/nyas.13865, 2019.

Magny, M., Combourieu-Nebout, N., de Beaulieu, J. L., Bout- Roumazeilles, V., Colombaroli, D., Desprat, S., Francke, A.,
685 Joannin, S., Ortu, E., Peyron, O., Revel, M., Sadori, L., Siani, G., Sicre, M. A., Samartin, S., Simonneau, A., Tinner, W.,
Vannière, B., Wagner, B., Zanchetta, G., Anselmetti, F., Brugiapaglia, E., Chapron, E., Debret, M., Desmet, M., Didier, J.,
Essallami, L., Galop, D., Gilli, A., Haas, J. N., Kallel, N., Millet, L., Stock, A., Turon, J. L., and Wirth, S.: North-south
palaeohydrological contrasts in the central Mediterranean during the Holocene: tentative synthesis and working hypotheses,
Clim. Past, 9, 2043– 2071, doi:10.5194/cp-9-2043, 2013.
690
Masson, V., Cheddadi, R., Braconnot, P., Joussaume, S., Texier, D., and participants, P.M.I.P.: Mid-Holocene climate in
Europe: what can we infer from PMIP model data, 1999.

Mauri, A., Davis, B. A. S, Collins, P., and Kaplan, J. O.: The climate of Europe during the Holocene: a gridded pollen-based
695 reconstruction and its multi-proxy evaluation. Quaternary Science Reviews, 112, 109-127, 215, 2015.

Mauri, A., Davis, B. A. S., Collins, P. M., and Kaplan, J. O.: The influence of atmospheric circulation on the mid Holocene
climate of Europe: a data-model comparison, 2014.

700 Murphy, J.: An evaluation of statistical and dynamical techniques for downscaling local climate. *J. Climate,* **12,** 2256–2284,
1999.

Opsteegh, J. D., Haarsma, R. J., Selten, F. M., and Kattenberg, A.: ECBILT: a dynamic alternative to mixed boundary
conditions in ocean models, Tellus A, 50, 348–367, https://doi.org/10.1034/j.1600-0870.1998.t01-1-00007.x, 1998.
705
Otto-Bliesner, B. L., Brady, E. C., Tomas, R., Levis, S., and Kothavala, Z.: Last Glacial Maximum and Holocene climate in
CCSM3. Journal of Climate 19, 2526–2544, 2006.

Peyron, O., Combourieu-Nebout, N., Brayshaw, D., Goring, S., Andrieu-Ponel, V., Desprat, S., Fletcher, W., Gambin, B.,
710 Ioakim, C., Joannin, S., Kotthoff, U., Kouli, K., Montade, V., Pross, J., Sadori, L., and Magny, M.: Precipitation changes in
the Mediterranean basin during the Holocene from terrestrial and marine pollen records: a model–data comparison, Clim. Past,
13, 249–265, https://doi.org/10.5194/cp-13-249-2017, 2017.
.

Quiquet, A., Roche, D. M., Dumas, C., and Paillard, D.: Online dynamical downscaling of temperature and precipitation within
715 the iLOVECLIM model (version 1.1). *Geoscientific Model Development*, *11*(1), 453–466. https://doi.org/10.5194/gmd-11-
453-2018, 2018.

Raible, C. C., Bärenbold, O., and Gómez-navarro, J. J.: Drought indices revisited–improving and testing of drought indices in
a simulation of the last two millennia for Europe. *Tellus A Dyn.Meteorol. Oceanogr.* **69:** 1287492, 2017.
720

Raynaud, D., Barnola, JM., Chappellaz, J., Blunier, T., Indermuhle, A., and Stauffer, B.: The ice record of greenhouse gases:
a view in the context of future changes. Quat Sci Rev 19:9–17, 2000.

Renssen, H., and Osborn, T. J.: Investigating Holocene climate variability: data-model comparisons. PAGES News, 11 (2-3),
725 32-33, 2003.

Renssen, H., Goosse, H., Fichefet, T., Brovkin, V., Driesschaert, E., and Wolk, F.: Simulating the Holocene climate evolution
at northern high latitudes using a coupled atmospheresea ice-ocean-vegetation model, Clim. Dynam., 24, 23–43,
doi:10.1007/s00382-004-0485-y, 2005a.

730 Renssen, H., Goosse, H., and Fichefet, T.: Contrasting trends in North Atlantic deep-water formation in the Labrador and
Nordic Seas during the Holocene. Geophysical Research Letters 32, doi 10.1029/2005GL022462, L08711, 2005b.

Renssen, H., Isarin, R., Jacob, D. J., Podzun, R., and Vandenberghe, J.: Simulation of the Younger Dryas climate in Europe
using a regional climate model nested in an AGCM: preliminary results. *Global and Planetary Change, 30*, 41-57, 2001.
735

Roberts, N., Brayshaw, D., Kuzucuoğlu, C., Perez, R., and Sadori, L.: The mid-Holocene climatic transition in the
Mediterranean: Causes and consequences, The Holocene, 21, 3–13, 2011.

Roche, D. M., Dokken, T. M., Goosse, H., Renssen, H., and Weber, S. L.: Climate of the Last Glacial Maximum: sensitivity
740   studies and model-data comparison with the LOVECLIM coupled model, Clim. Past, 3, 205–224, https://doi.org/10.5194/cp-
3-205, 2007.

Roche, D. M., Dumas, C., Bügelmayer, M., Charbit, S., and Ritz, C.: Adding a dynamical cryosphere to iLOVECLIM (version
1.0): coupling with the GRISLI ice-sheet model, Geosci. Model Dev., 7, 1377–1394, https://doi.org/10.5194/gmd-7-1377,
745   2014.

Russo, E., and Cubasch, U.: Mid-to-late Holocene Temperature Evolution and Atmospheric Dynamics over Europe in Regional
Model Simulations. Climate of the Past Discussions. 1-24. 10.5194/cp-2016-10, 2016.

750   Sadori, L., Giraudi, C. Masi, A., Magny, M., Ortu, E., Zanchetta, G., and Izdebski, A.: Climate, environment, and society in
southern Italy during the last 2000 years. A review of the environmental, historical and archaeological evidence, Quaternary
Science Reviews, 136, 798 173-188, 2016.

Schaeffer, M., Selten, F., Goosse, H., and Opsteegh, T.: On the influence of location of high-latitude ocean deep convection
755   and Arctic sea-ice on climate change projections, J. Climate, 17(22), 4316–4329, 2004.

Schaeffer, M., Selten, F. M., Goosse, H., and Opsteegh, J. D.: Limited predictability of regional climate change in IPCC SRES
scenarios. Geophysical Research Letters, 29, 16, 10.1029/2002GL015254, 2002.

Schilt, A., Baumgartner, M., Schwander, J., Buiron, D., Capron, E., Chappellaz, J., Loulergue, L., Schüpbach, S., Spahni, R.,
760   Fischer, H., and Stocker, T. F.: Atmospheric nitrous oxide during the last 140,000years. Earth Planet Sc. Lett. 300, 33e43.
http://dx.doi.org/10.1016/j.epsl.2010.09.027, 2010.

Schmidt, G. A., Shindell, D. T., Miller, R. L., Mann, M. E., and Rind, D.: General circulation modelling of Holocene climate
variability. Quaternary Science Reviews 23, 2167–2181, 2004.
765

Seppä H., and Birks H. J. B.: July mean temperature and annual precipitation trends during the Holocene in the Fennoscandian
tree-line area: pollen-based climate reconstructions. The Holocene; 11(5):527-539. doi:10.1191/095968301680223486, 2001.

Stoner, A. M. K., Hayhoe, K., Yang, X. and Wuebbles, D. J.: An asynchronous regional regression model for statistical
770   downscaling of daily climate variables. Int. J. Climatol., 33: 2473-2494. https://doi.org/10.1002/joc.3603, 2013

Strandberg, G., J. Brandefelt, E., Kjellstrom and Smith, B.: High-resolution regional simulation of last glacial maximum climate in Europe. Tellus A Dyn. Meteorol. Oceanogr. 63: 107–125, 2011.

775 Timm, O., Timmermann, A., Abe-Ouchi, A., Saito, F., and Segawa, T.: On the definition of seasons in paleoclimate simulations with orbital forcing, Paleoceanography, 23, PA2221, doi:10.1029/2007PA001461, 2008.

Timmermann, A., Justino Barbosa, F., Jin, F.F., and Goosse, H.: Surface temperature control in the North Pacific during the last glacial maximum. Climate Dynamics, 23, doi 10.1007/s00382-004-0434-9, 353-370. of Intermediate Complexity: closing the gap in the spectrum of climate system models, Clim. Dynam., 18, 579–586, 2004.

780
Viner, D.: Spatial Downscaling: retrieved from http://www.cccsn.ec.gc.ca/?page=downscaling, 2012.

Wang, J., Swati, F. N. U., Stein, M. L. and Kotamarthi, V. R.: Model performance in spatiotemporal patterns of precipitation: New methods for identifying value added by a regional climate model. *J. Geophys. Res. Atmos.*, 120: 1239– 1259.
785 doi: 10.1002/2014JD022434, 2015.

Wanner, H., Beer, J., Bütikofer, J., Crowley, T. J., Cubasch, U., Flückiger, J., Goosse, H., Grosjean, M., Joos, F., Kaplan, J. O., Küttel, M., Müller, S. A., Prentice, I. C., Solomina, O., Stocker, T. F., Tarasov, P. E., Wagner, M., and Widmann, M.: Mid- to late Holocene climate change – an overview, Quaternary Sci. Rev., 27, 1791–1828, 2008.

790
Wu, H. B., Guiot, J. L., Brewer, S., and Guo, Z. T.: Climatic changes in Eurasia and Africa at the last glacial maximum and mid-Holocene: reconstruction from pollen data using inverse vegetation modelling. Clim. Dyn. 29, 211e229, 2007.

Yokoyama, Y., Lambeck, K., De Deckker P, Johnston, P., and Fifield, L. K.: Timing of the Last Glacial Maximum from
795 observed sea-level minima. *Nature*, *406*(6797), 713–716. https://doi.org/10.1038/35021035, 2000.

Zhang Y, Renssen H, and Seppä H.: Effects of melting ice sheets and orbital forcing on the early Holocene warming in the extratropical Northern Hemisphere. *Climate of the Past* **12**: 1119–1135, 2016.

800 Zhang, Y., Renssen, H., Seppä, H., and Valdes, P. J.; Holocene temperature trends in the extratropical Northern Hemisphere based on inter-model comparisons. *Journal of Quaternary Science*, *33*(4), 464-476. https://doi.org/10.1002/jqs.3027, 2018.

Zorita, E., Gonz´alez-Rouco, J. F., von Storch, H., Mont´avez, J. P., and Valero, F.: Natural and anthropogenic modes of surface temperature variations in the last thousand years, Geophys. Res. Lett., 32, 755–762, 2005.